International Journal of Physical Sciences

Volume 11 Number 12 30 June , 2016

ISSN 1992-1950

Academic Journals

ABOUT IJPS

The **International Journal of Physical Sciences (IJPS)** is published weekly (one volume per year) by Academic Journals.

International Journal of Physical Sciences (IJPS) is an open access journal that publishes high-quality solicited and unsolicited articles, in English, in all Physics and chemistry including artificial intelligence, neural processing, nuclear and particle physics, geophysics, physics in medicine and biology, plasma physics, semiconductor science and technology, wireless and optical communications, materials science, energy and fuels, environmental science and technology, combinatorial chemistry, natural products, molecular therapeutics, geochemistry, cement and concrete research, metallurgy, crystallography and computer-aided materials design. All articles published in IJPS are peer-reviewed.

Contact Us

Editorial Office: ijps@academicjournals.org

Help Desk: helpdesk@academicjournals.org

Website: http://www.academicjournals.org/journal/IJPS

Submit manuscript online http://ms.academicjournals.me/

Editors

Editorial Board

International Journal of Physical Sciences

Table of Contents: Volume 11 Number 12, 30 June, 2016

ARTICLES

academicJournals

Vol. 11(12), pp. 144-148, 30 June, 2016
DOI: 10.5897/IJPS2015.4423
Article Number: D0DE8D159509
ISSN 1992 - 1950

http://www.academicjournals.org/IJPS

International Journal of Physical Sciences

Full Length Research Paper

Geometric phases for two-mode squeezed vacuum state

Da-Bao Yang[1]* and Ji-Xuan Hou[2]

[1]Department of Fundamental Physics, School of Science, Tianjin Polytechnic University, Tianjin 300387, People's Republic of China.
[2]Department of Physics, Southeast University, Nanjing 211189, People's Republic of China.

Received 7 October, 2015; Accepted 20 May, 2016

Although the geometric phase for one-mode squeezed state had been studied in detail, the counterpart for two-mode squeezed state is vacant. In this paper, we aim at the special case, namely, two-mode squeezed vacuum state. Furthermore, the total phase factor is to be written in an elegant form, which is just identical to one term of product of two squeezed operators. In addition, when this system undergoes cyclic evolutions, the corresponding geometric phase is obtained, which is the sum of the counterparts of two isolated one-mode squeezed vacuum state. Finally, the relationship between the cyclic geometric phase and entanglement of two-mode squeezed vacuum state is established.

Key words: Quantum optics, Geometric phases, Entanglement

INTRODUCTION

Squeezed light plays an important role in the development of quantum optics (Walls, 1983). It preserves the minimum uncertainty and exhibits non-classical nature of light, such as sub-Poissonian statistics which can be observed as photon antibunching effect. It also has many applications in optical communications and detection of gravitational radiation. It was be generalized to nonlinear case (Kwek and Kiang, 2003). But their studies were just confined to one mode case. Moreover, two mode squeezed state was systematically studied (Caves and Schumaker, 1985; Schumaker and Caves, 1985).

Since geometric phase had been discovered (Berry, 1984) in the quantum system which underwent adiabatic and unitary evolution, its research exploded. Subsequently, It was extended to non-Abelian case (Wilczek and Zee, 1984). Its non-adiabatic and cyclic counterpart was studied (Aharonov and Anandan, 1987; Anandan, 1988). Soon, by getting rid of the condition of cyclic evolution, it was generalized to a more general case (Samuel and Bhandari, 1988), which depended on the earlier study (Pancharatnam, 1956). Subsequently, using kinematic approach, geometric phase was derived as well (Mukunda and Simon, 1993).

Moreover, the geometric phases also had other generalizations, such as off-diagonal ones (Kult, 2007; Manini and Pistolesi, 2000; Mukunda et al., 2001) and mixed state counterparts (Singh et al., 2003; Sjoqvist et al., 2000; Tong et al., 2004).

In addition, geometric phases also have many applications, which range from quantum information and

*Corresponding author. Email: bobydbcn@163.com.

PACS: 42.50.-p, 03.65.Vf, 03.67.Bg

computation science (Duan et al., 2001; Jones et al., 2000) to condensed matter (Xiao et al., 2010). Also, this subject is introduced elaborately by many monographs (Bohm et al., 2003; Chruściński and Jamiołkowski, 2004; Wilczek and Shapere, 1989).

Meanwhile, the interdisciplinary study between quantum optics and geometric phase has also emerged. Berry phase for coherent and squeezed states was researched (Chaturvedi et al., 1987); the non-adiabatic geometric phase for squeezed state was studied by Liu et al. (1998); the geometric phase for nonlinear coherent and squeezed state in kinematic approach was discussed (Yang et al., 2011). However, the above studies are all confined to one-mode case. In seeking for theoretical progress, the two-mode case will be researched in this paper. Moreover, the degree of entanglement between the two-mode state is to be evaluated.

This paper is organized as follows. First is a presentation of the features of two-modes squeezed states followed by a review of the kinematic approach to geometric phase. Next, the geometric phase for two-mode squeezed state was calculated. From the above outcome, when the system undergoes cyclic evolution, the corresponding result was also obtained. Moreover, the Von Neumann entropy was calculated, and its relation with geometric phase established. Finally, the research was concluded.

REVIEW OF TWO-MODE SQUEEZED VACUUM STATES AND GEOMETRIC PHASES

The Hamiltonian for two-mode of electromagnetic field (Schumaker and Caves, 1985) takes the form

$$H_0 = \Omega(a_+^\dagger a_+ + a_-^\dagger a_-) + \varepsilon(a_+^\dagger a_+ - a_-^\dagger a_-), \tag{1}$$

where $\Omega \pm \varepsilon$ are the frequencies for the two-mode; also, we take $\hbar = 1$ for simplicity. Furthermore, Ω and ε can be regarded as a carrier frequency and a modulation frequency respectively. And the electromagnetic field are quantized by the following commutation relations

$$[a_+, a_-] = [a_+^\dagger, a_-^\dagger] = 0$$

$$[a_+, a_+^\dagger] = [a_-, a_-^\dagger] = 1.$$

The squeezed operator (Schumaker and Caves, 1985) is generalized as

$$S(r,\phi) \equiv \exp[r(a_+ a_- e^{-2i\phi} - a_+^\dagger a_-^\dagger e^{2i\phi})], \tag{2}$$

where the real number r is called the squeeze factor and ϕ is a real phase angle. Moreover, the above operator (2) is unitary,

$$S^{-1}(r,\phi) = S^\dagger(r,\phi) = S(-r,\phi).$$

Hence, the squeezed vacuum state is

$$S(r,\phi)\,|\,0\rangle \tag{3}$$

Under the Hamiltonian (1), it evolves as

$$\begin{aligned} e^{-iH_0 t} S(r,\phi)\,|\,0\rangle &= e^{-iH_0 t} S(r,\phi) e^{iH_0 t}\,|\,0\rangle \\ &= S(r,\phi - \Omega t)\,|\,0\rangle \end{aligned} \tag{4}$$

which uses the following formulas (Schumaker and Caves, 1985)

$$\exp[-i\varepsilon t(a_+^\dagger a_+ - a_-^\dagger a_-)] S(r,\phi) \exp[i\varepsilon t(a_+^\dagger a_+ - a_-^\dagger a_-)] = S(r,\phi)$$

and

$$\exp[-i\theta(a_+^\dagger a_+ + a_-^\dagger a_-)] S(r,\phi) \exp[i\theta(a_+^\dagger a_+ + a_-^\dagger a_-)] = S(r,\phi - \theta).$$

The geometric phases γ (Mukunda and Simon, 1993) for arbitrary time t takes the form

$$\gamma = \arg\langle\psi(0)|\psi(t)\rangle + \int_0^t \langle\psi(\tau)|H|\psi(\tau)\rangle d\tau. \tag{5}$$

It is a physical reality, due to it is invariant under gauge transformation. And it can be explained as an outcome of parallel transportation in the framework of fiber bundle, that is, holonomy, hence it is fittingly called geometric phase.

EVALUATIONS OF THE GEOMETRIC PHASE FACTOR

For convenience, instead of calculating the geometric phase, we evaluate the geometric phase factor,

$$e^{i\gamma} = \frac{\langle\psi(0)|\psi(t)\rangle}{\|\langle\psi(0)|\psi(t)\rangle\|} e^{i\delta}, \tag{6}$$

where

$$\delta = \int_0^t \langle\psi(\tau)|H|\psi(\tau)\rangle d\tau \tag{7}$$

which is identical to negative the dynamical phase.

At first, let us calculate the inner product

$$\begin{aligned} \langle\psi(0)|\psi(t)\rangle &= \langle 0\,|\,S^\dagger(r,\phi) e^{-iH_0 t} S(r,\phi)\,|\,0\rangle \\ &= \langle 0\,|\,S^\dagger(r,\phi) S(r,\phi - \Omega t)\,|\,0\rangle, \end{aligned} \tag{8}$$

which uses Equation (4). In order to work out the total phase, the following formula (Schumaker and Caves, 1985) is very useful

$$S^{\dagger}(r',\phi')S(r'',\phi'')=e^{-i\Theta}S(R,\Phi-\Theta)U(\Theta), \quad (9)$$

where the above parameters satisfy the matrix equation

$$C_{R,\Phi}e^{i\Theta\sigma_3}=C_{r'',\phi''}C_{-r',\phi'}, \quad (10)$$

where the matrix $C_{r,\phi}$ is defined by

$$C_{r,\phi}=\begin{pmatrix}\cosh r & e^{2i\phi}\sinh r\\ e^{-2i\phi}\sinh r & \cosh r\end{pmatrix} \quad (11)$$

and σ_3 is the famous Pauli matrix in the z direction. By substituting Equation 9 into Equation 8, one obtains

$$\langle\psi(0)|\psi(t)\rangle=\langle 0|e^{-i\Theta}S(R,\Phi-\Theta)U(\Theta)|0\rangle,$$

where

$$U(\Theta)=exp[-i\Theta(a_+^{\dagger}a_+ + a_-^{\dagger}a_-)].$$

By use of the explicit decomposition of squeezed operator (Schumaker and Caves, 1985):

$$S(R,\Psi)=(\cosh R)^{-1}e^{-a_+^{\dagger}a_-^{\dagger}e^{2i\Psi}\tanh R}e^{-(a_+^{\dagger}a_+ + a_-^{\dagger}a_-)\ln(\cosh R)}e^{a_+a_-e^{-2i\phi}\tan R}, \quad (12)$$

the total phase can be transformed to be an elegant manner

$$\langle\psi(0)|\psi(t)\rangle=(\cosh R)^{-1}e^{-i\Theta}, \quad (13)$$

of which parameters are determined by Equation (10). Its explicit form is

$$\begin{pmatrix}e^{i\Theta}\cosh R & e^{i(2\Phi-\Theta)\sinh R}\\ e^{i(\Theta-2\Phi)}\sinh R & e^{-i\Theta}\cosh R\end{pmatrix}=\begin{pmatrix}e^{-i\Omega t(i\cosh 2r\sin\Omega t+\cos\Omega t)} & e^{i(2\phi-\Omega t-\pi/2)}\sinh 2r\sin\Omega t\\ e^{-i(2\phi-\Omega t-\pi/2)}\sinh 2r\sin\Omega t & e^{i\Omega t}(\cos\Omega t-i\sin\Omega t\cosh 2r)\end{pmatrix}.$$

Therefore, the element $(2,2)$ can tell us the total phase factor $e^{-i\Theta}$, which take the form

$$\frac{e^{i\Omega t}(\cos\Omega t-i\sin\Omega t\cosh 2r)}{(\cos^2\Omega t+\sin^2\Omega t\cosh^2 2r)^{1/2}}. \quad (14)$$

Moreover, let us calculate another term δ (7) in the expression of geometric phase (5). By substituting Equation 4 into Equation 7, one can obtain

$$\delta=\int_0^t\langle 0|S^{\dagger}(r,\phi-\Omega\tau)HS(r,\phi-\Omega\tau)|0\rangle d\tau.$$

By use of the following formulas (Schumaker and Caves, 1985)

$$\begin{aligned}S^{\dagger}(r,\eta)a_+S(r,\eta) &= a_+\cosh r-a_-^{\dagger}e^{2i\eta}\sinh r\\ S^{\dagger}(r,\eta)a_-S(r,\eta) &= a_-\cosh r-a_+^{\dagger}e^{2i\eta}\sinh r,\end{aligned}$$

the formula for δ can be simplified as

$$\delta=2\Omega t\sinh^2 r. \quad (15)$$

Finally, by inserting Equations 14 and 15 into Equation 6, the geometric phase is achieved as

$$e^{i\gamma}=\frac{e^{i\Omega t\cosh 2r}(\cos\Omega t-i\sin\Omega t\cosh 2r)}{(\cos^2\Omega t+\sin^2\Omega t\cosh^2 2r)^{1/2}}$$

Now, the cyclic geometric phase will be discussed. From the total phase factor (8), it is not hard to see that when $\Omega t=2\pi$, the state (4) will undergo a genuine cyclic evolution of which the final state is exactly the initial state. In other words, the total phase can be regarded as zero. Hence the geometric phase can by explicitly expressed

$$\gamma_c=4\pi\sinh^2 r \quad mod \quad 2\pi, \quad (16)$$

which is exactly negative the dynamical phase. Because total phase vanish and the geometric phase is equal to the difference between the total phase and dynamical phase along with Yang et al. (2011), the geometric phase for isolated one-mode squeezed state is

$$\gamma_{ic}=2\pi\sinh^2 r \quad mod \quad 2\pi,$$

where the subscript index i implies mode. So if we define cyclic geometric phase to the simplest form, in combination with Equation 16, $\gamma_c=\gamma_{1c}+\gamma_{2c}$, which reveals the additional relationship between the two-mode system and the isolated one mode system.

Moreover, the cyclic geometric phase γ_c is related to the Von Neumann entropy which can measure the entanglement between the two modes in the squeezed state. In order to establish the relationship. Let us calculate the entropy first. By use of Equation 12,

$$S(r,\phi-\Omega t)|0\rangle=\frac{1}{\cosh r}\sum_{n=0}^{\infty}(-e^{2i(\phi-\Omega t)}\tanh r)^n|n\rangle_+|n\rangle_-.$$

Fortunately, it is already in the form of Schmidt decomposition. By a brute force calculation, the Von Neumann entropy reads

$$E=\cosh^2 r\ln(\cosh^2 r)-\sinh^2 r\ln\sinh^2 r, \quad (17)$$

which is identical to the result in Van Enk (1999). Finally,

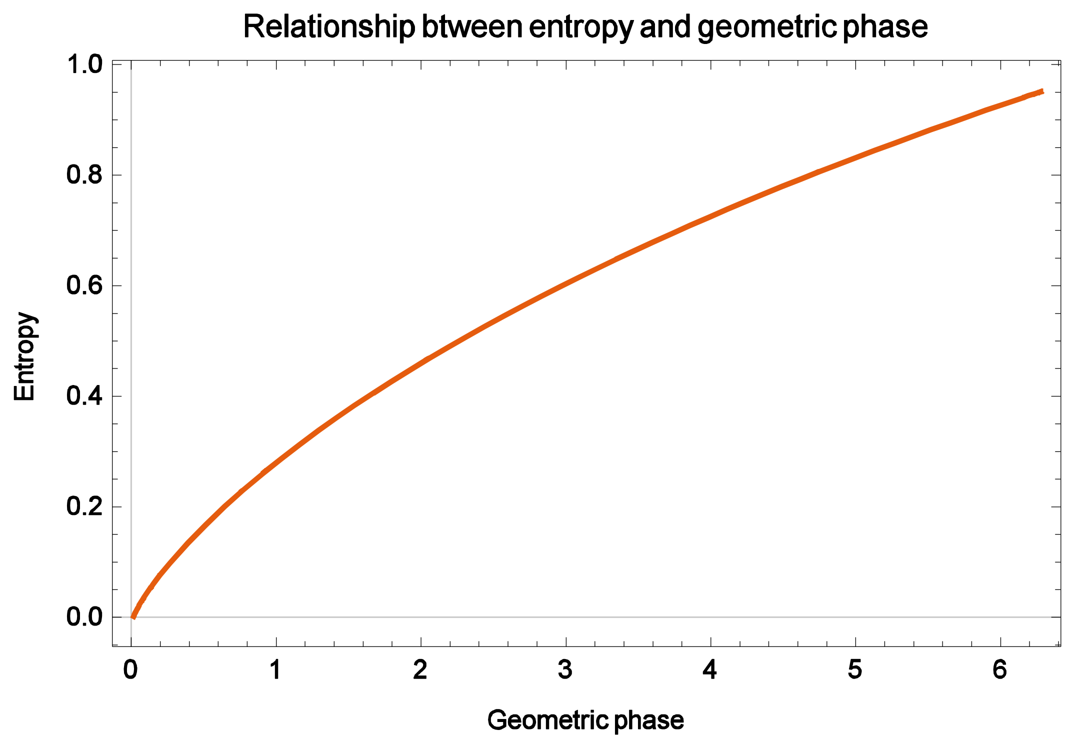

Figure 1. γ_c is set to vary from 0 to 2π.

substituting Equation 16 into Equation 17, we obtain

$$E = (1+\frac{\gamma_c}{4\pi})\ln(1+\frac{\gamma_c}{4\pi}) - \frac{\gamma_c}{4\pi}\ln\frac{\gamma_c}{4\pi},$$

which shows the relationship between the entanglement and the cyclic geometric phase. And the corresponding graph is as shown in Figure 1.

Conclusions

In this article, the geometric phase factor for two-mode squeezed vacuum state is evaluated explicitly. The total phase factor (13) is turned to be an elegant outcome, which is just one term of the product of the initial squeezed operator and final squeezed operator (9). When this system undergoes cyclic evolutions, the corresponding geometric phase is obtained, which is just the sum of the counterparts of two isolated one-mode squeezed state. Furthermore, the relationship between the cyclic geometric phase and entanglement of two-mode squeezed state is established.

Conflict of Interests

The authors have not declared any conflict of interest.

ACKNOWLEDGEMENTS

D.B.Y. is supported by NSF of China under Grant No. 11447196. And J.X.H. is supported by the NSF of China under Grant 11304037, the NSF of Jiangsu Province, China under Grant BK20130604, as well as the Ph.D. Programs Foundation of Ministry of Education of China under Grant 20130092120041.

REFERENCES

Aharonov Y, Anandan A (1987). Phase change during a cyclic quantum evolution. Phys. Rev. Lett. P 58.
Anandan J (1988). Non-adiabatic non-abelian geometric phase. Phys. Lett. A 133:171-175.
Berry MV (1984). Quantal phase factors accompanying adiabatic changes. Proc. R. Soc. London Ser. A 392:45-57.
Bohm A, Mostafazadeh A, Koizumi H, Niu Q, Zwanziger J (2003). The geometric phase in quantum systems (Springer-Verlag, Berlin, 2003).
Caves CM, Schumaker BL (1985). New Formalism for Two-photon Quantum Optics. I. Quadrature Phases and Squeezed States. Phys. Rev. A 31:3068-3092.
Chaturvedi S, Sriram M, Srinivasan V (1987). Berry's phase for coherent states. J. Phys. A 20:L1071.
Chruściński D, Jamiołkowski A (2004). Geometric phases in classical and quantum mechanics (Birkhauser, New York, 2004).
Duan LM, Cirac J, Zoller P (2001). Geometric manipulation of trapped ions for quantum computation. Science 292:1695.
Jones JA, Vedral V, Ekert A, Castagnoli G (2000). Geometric quantum computation using nuclear magnetic resonance. Nature 403:869-871.
Kult D (2007). Non-Abelian generalization of off-diagonal geometric phases. Europhys. Lett. 78:60004.

Kwek L, Kiang D (2003). Nonlinear Squeezed States. J. Opt. B: Quan. Semi. Opt. 5:383.
Liu J, Hu B, Li B (1998). Nonadiabatic Geometric Phase and Hannay Angle: A Squeezed State Approach. Phys. Rev. Lett. 81:1749-1753.
Manini N, Pistolesi F (2000). Off-Diagonal Geometric Phases. Phys. Rev. Lett. 85:3067.
Mukunda N, Arvind R, Chaturvedi S, Simon R (2001). Bargmann invariants and off-diagonal geometric phases for multilevel quantum systems: A unitary-group approach. Phys. Rev. A 65:012102.
Mukunda N, Simon R (1993). Quantum kinematic approach to the geometric phase. I. General formalism. Ann. Phys. 228:205-268.
Pancharatnam S (1956). Generalized theory of interference and its applications. Paper presented at the Proceedings of the Indian Academy of Sciences-Section A.
Samuel J, Bhandari R (1988). General Setting for Berry's Phase. Phys. Rev. Lett. 60:2339.
Schumaker BL, Caves CM (1985). New formalism for two-photon quantum optics. II. Mathematical foundation and compact notation. Phys. Rev. A 31:3093-3111.
Singh K, Tong DM, Basu K, Chen JL, Du JF (2003). Geometric phases for nondegenerate and degenerate mixed states. Phys. Rev. A 67:032106.
Sjoqvist E, Pati AK, Ekert A, Anandan JS, Ericsson M, Oi DKL, Vedral V (2000). Geometric phases for mixed states in interferometry. Phys. Rev. Lett. 85:2845.
Tong DM, Sjoqvist E, Kwek LC, Oh CH (2004). Kinematic Approach to the Mixed State Geometric Phase in Nonunitary Evolution. Phys. Rev. Lett. 93:080405.
Van Enk S (1999). Discrete formulation of teleportation of continuous variables. Phys. Rev. A 60:5095.
Walls DF (1983). Squeezed States of Light. Nature 306:141-146.
Wilczek F, Shapere A (1989). Geometric phases in physics (World Scientific, Singapore, 1989.
Wilczek F, Zee A (1984). Appearance of gauge structure in simple dynamical systems. Phys. Rev. Lett. 52:2111-2114.
Xiao D, Chang M-C, Niu Q (2010). Berry phase effects on electronic properties. Rev. Mod. Phys. 82:1959-2007.
Yang DB, Chen Y, Zhang FL, Chen JL (2011). Geometric phases for nonlinear coherent and squeezed states. J. Phys. B 44:075502.

academicJournals

Vol. 11(12), pp. 149-156, 30 June, 2016
DOI: 10.5897/IJPS2016.4508
Article Number: F99DFA159511
ISSN 1992 - 1950

http://www.academicjournals.org/IJPS

International Journal of Physical Sciences

Full Length Research Paper

Preliminary structural evaluation of an X-Field Onshore Niger Delta using 3D seismic data

C. N. Ehirim* and M. A. E. Abbey

Geophysics Research Group, Department of Physics, University of Port Harcourt, P. O. Box 122, Choba, Port Harcourt, Nigeria.

Received 23 May, 2016; Accepted 20 June, 2016

A structural evaluation of a post stack time migrated (PSTM) 3D seismic data over an X–Field in the eastern Niger Delta has been attempted. The objective of the study is to structurally evaluate the field with a view to identifying structural features such as faults, map geologic horizons and analyze reflection characteristics that might be a good lead to probable hydrocarbon accumulations. Results revealed that six growth faults (F_1, F_2, F_3, F_4, F_5, and F_6) and three seismic horizons (H_I, H_2 and H_3) were delineated on the seismic section. F_1, F_2, F_4, F_5 and F_6 are synthetic, while F_3 is antithetic growth faults. The synthetic faults trend northeast-southwest and dips southwestward, while the antithetic fault trend northwest-southeast and dips southeastward. The seismic horizons are fault truncated with hanging wall/footwall fault assisted closures characterized by distinctive high amplitude reflection events. The horizons have good reflection continuity, moderate to strong reflection strength and medium to high amplitudes. These suggests wide spread and uniform deposition of clastic sediments with thick sand facies and inter-bedding shales, which is the characteristic of a hydrocarbon reservoir in the Niger Delta basin. The potential for hydrocarbons is high in this prospect field based on our preliminary study, which could be explored.

Key words: Growth faults, seismic horizons, fault closures, post stack time migrated (PSTM) 3D seismic data.

INTRODUCTION

Niger Delta is an inland tertiary sedimentary basin characterized by structural and stratigraphic complexities consequent from its formational stages and development. As a result, the search for oil and gas has become increasingly difficult and challenging in the face of these complexities because of problems associated with seismic imaging of subsurface structures associated with hydrocarbon accumulations. These complexities of the delta can be evaluated by the structural interpretation of 3D seismic data. Structural analysis of seismic data is the key to reservoir evaluation and has become the main tool in the exploration and management of hydrocarbon reservoirs (Bahorich and Farmer, 1995; Sheriff and Geldart, 1995).

Seismic interpretation involves determining the geologic significance of seismic data. The basic goal remains identifying likely hydrocarbon accumulations based on structure to reduce drilling risk. This begins with structural

*Corresponding author. E-mail: emekabridgy@yahoo.com.

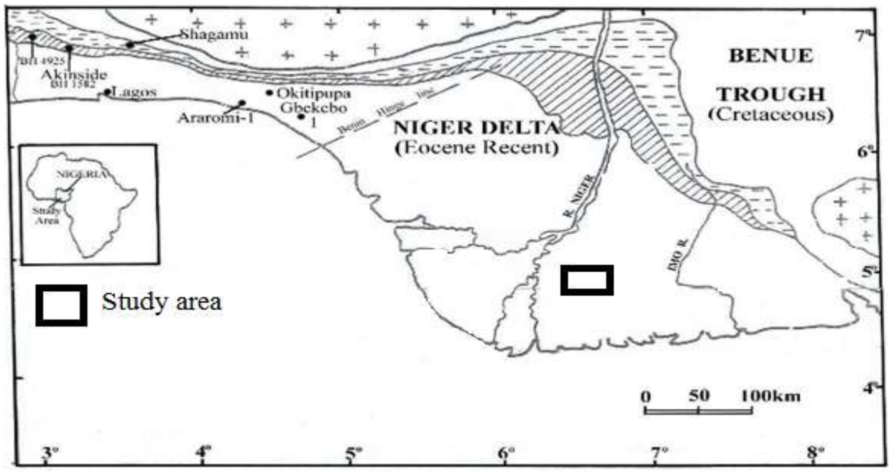

Figure 1. Location map of the study area (Adapted with modifications from Petters and Olsson (1979).

mapping of reservoir parameters such as faults, horizon depth, reservoir thickness, lithology and dip of the reservoir bed. Structural interpretation of 3D seismic data entails identifying, picking and tracking of laterally consistent seismic reflectors for the primary objective of mapping geologic structures, depth of primary reflector, stratigraphy and perhaps to probe reservoir architecture (Anstey, 1980; Mcquillin et al., 1984; Allstair, 2011; Avseth et al., 2005). The appropriate end result would be to detect possible hydrocarbon traps, delineate their extent and calculate their volumes.

Several authors have attempted structural interpretation in the Niger Delta using seismic data (Ogboke, 2006; Oyedele et al., 2013; Obiekezie, 2014; Odoh et al., 2014), for the primary purpose of evaluating stratigraphy and geologic structures and delineate traps with probable hydrocarbon accumulation. The authors reported that structural and stratigraphic information relating to hydrocarbon traps and accumulations can be derived from the detailed analysis of 3D seismic data.

The objective in this preliminary study is to structurally interpret a post stack time migrated (PSTM) 3D seismic data in the southern part of the X-Field by delineating and classifying faults, estimate their orientations and dips, map horizons and analyze reflection characteristics that may be associated with hydrocarbon accumulation in the field.

Location of the study area

The X-Field lies in the eastern swamp depobelt of the Niger Delta (Figure 1), over which a Post Stack Time Migrated (PSTM) 3D seismic data was acquired. Hydrocarbons are produced in the northern part of the field, while in the southern part production is yet to commence, which is the area of focus in the present study. The field is generally low-lying, flat and criss-crossed by dense network of meandering rivers and creeks with abundant rainfall. The vegetation is dominantly mangrove typical of the zone (Figure 1).

Geology of study area

The geology of the Niger Delta has been extensively and thoroughly discussed by several authors (Short and Stauble, 1967; Bouvier et al., 1989; Doust and Omatsola, 1990; Adejobi and Olayinka, 1997; Aigbedion and Iyayi, 2006; Ogboke, 2006). These authors were of the view that synsedimentary tectonics and associated sediment loading are responsible for the wealth of structural features that occur in the delta. These structural features are the mega-structural or depo belts, macro (growth faults and roll over anticlines) and diapiric structures (Figure 2) that are major determinant factors in the development of hydrocarbon habitat of the delta. These depobelts have synsedimentary faults which were formed in response to variable rates of sediment supply and subsidence. Each of the depobelts is a distinct unit which represents a break in regional dip of the delta and is bounded seaward by large counter-regional faults or the growth fault of the next seaward belt, and landward by growth faults.

The Niger Delta basin is underlain by three stratigraphic units, the top Benin Formation, the middle Agbada Formation and the deepest Akata Formation. The Benin Formation consists mainly of continental sand deposits with intercalation of shale and constitutes the main aquiferous unit of the basin. The formation is covered with topmost low velocity layer which, in most cases, is weathered within which surface waves are excited and generated. Immediately below the Benin Formation is the reservoir sand of the Agbada Formation which is believed

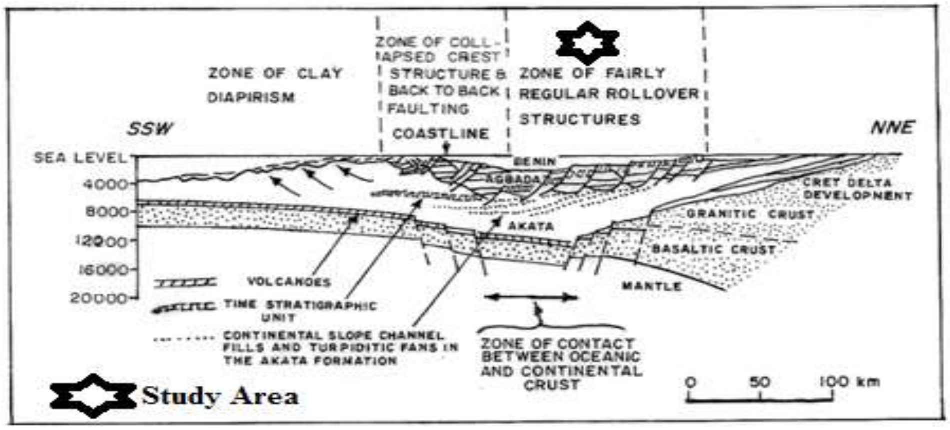

Figure 2. Tectonic and Geologic map of the Niger delta (After www.intechopen.com).

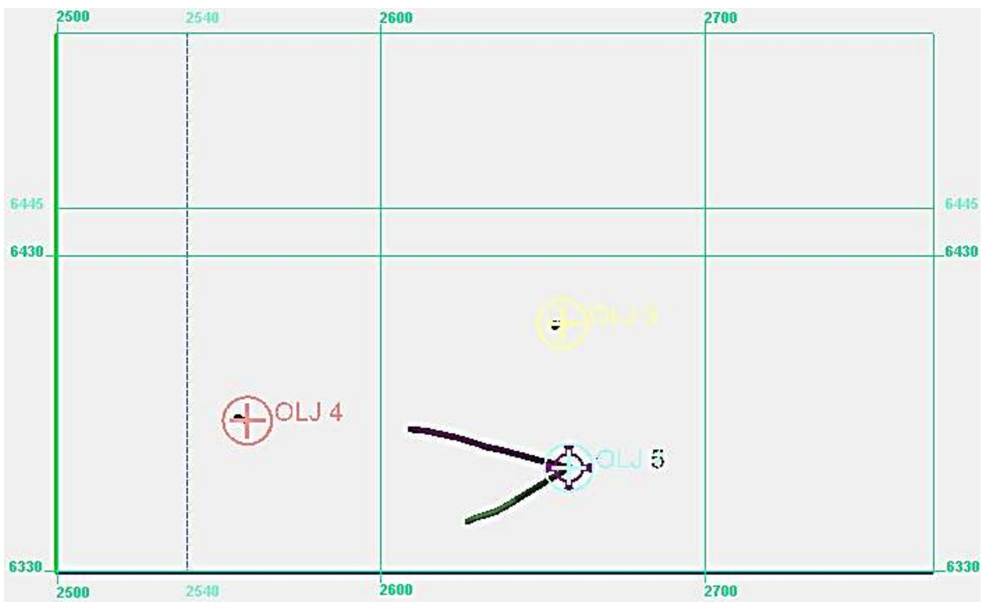

Figure 3. Seismic survey line of the study area.

to house the oil and gas resource of the Niger Delta. The Agbada Formation consists of unconsolidated to slightly consolidated paralic siliciclastic sequence of sandy unit with minor shale intercalations of about 4500 m thick (Weber and Daukoru, 1975). In the lower portion of the formation, shale and sandstone beds are deposited in equal proportion (50%), however, the upper section is mostly sand (75%) with minor shale intercalations. The Akata Formation at the base of the Delta is of marine origin and is composed of thick shale sequences (potential source rock), turbidite sand (potential reservoirs in deep water), and minor amounts of clay and silt. The formation underlies the entire delta, and is typically overpressured (Evamy et al., 1978; Doust and Omatsola, 1989).

METHODOLOGY

The data used in this study is a processed PSTM 3D seismic section acquired from an X-Field in the eastern Niger Delta field. The 3D data was acquired using split geometry on a brickwork acquisition pattern. This involves laying of the geophone and other accessories on the receiver lines and detonate explosives on the perpendicular source line to generate seismic energy, which is reflected and recorded on magnetic tape via the recording instrument. A source-receiver line spacings of 300 m, shot-receiver intervals of 50 m along the source - receiver lines, 24 m source depth and single shot dynamite was adopted (Figure 3). The acquisition was primarily targeted at a structure less than 2.6 s two way time (TWT), with a target bandwidth of 10 to 60 Hz.

The 3D PSTM reflection data was analyzed for fixed inline (2770) and varying cross lines (6250 to 6609) for fault interpretation and characterization, horizon mapping and attribute characterization (Figure 4). The identification of faults and mapping of seismic

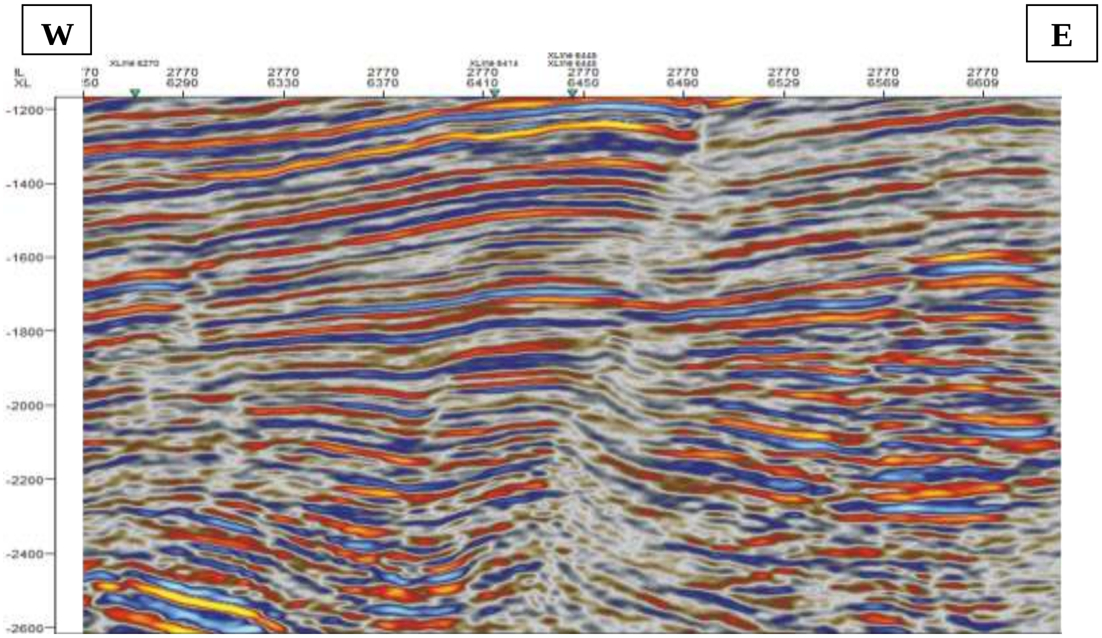

Figure 4. A 3D PSTM section of X- Field (In line 2770).

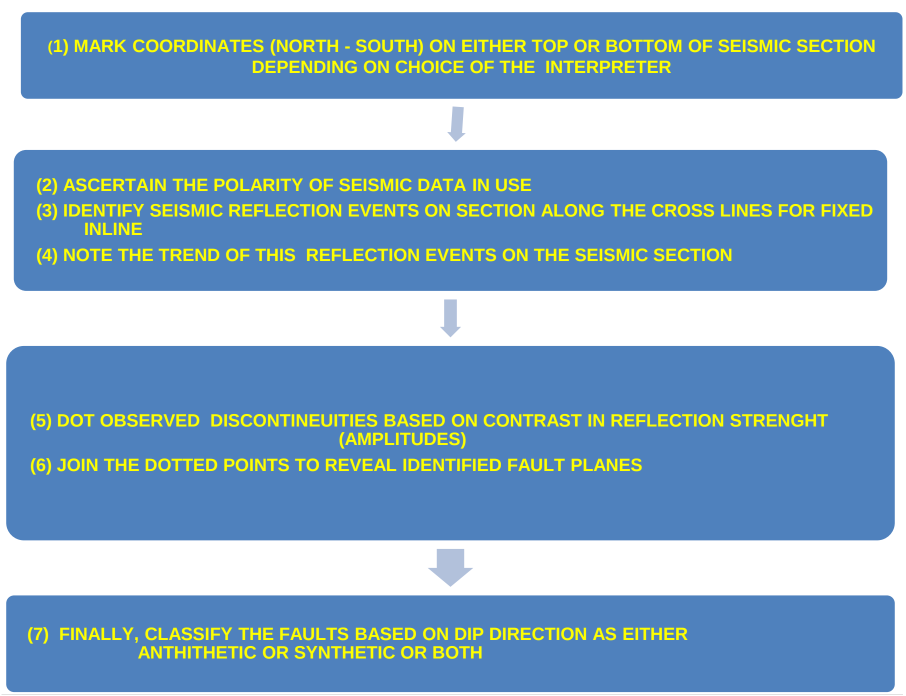

Figure 5. Workflow for the interpretation of the faults on the seismic section.

horizons were based on the work flows in Figures 5 and 6, respectively. This entails visually inspecting the seismic section for reflection discontinuities, vertical displacement of reflection events and abrupt termination of events, overlapping of reflections and changes in pattern and strength of reflection events across the seismic section. Based on this, faults are delineated, horizons are mapped across the section and the reflection characteristics of the section are analyzed in terms of reflection strength, amplitude, continuity and configuration.

PRESENTATION OF RESULTS

The field is an E-W elongate rollover anticline structure bounded by growth faults. It is both hanging wall/footwall

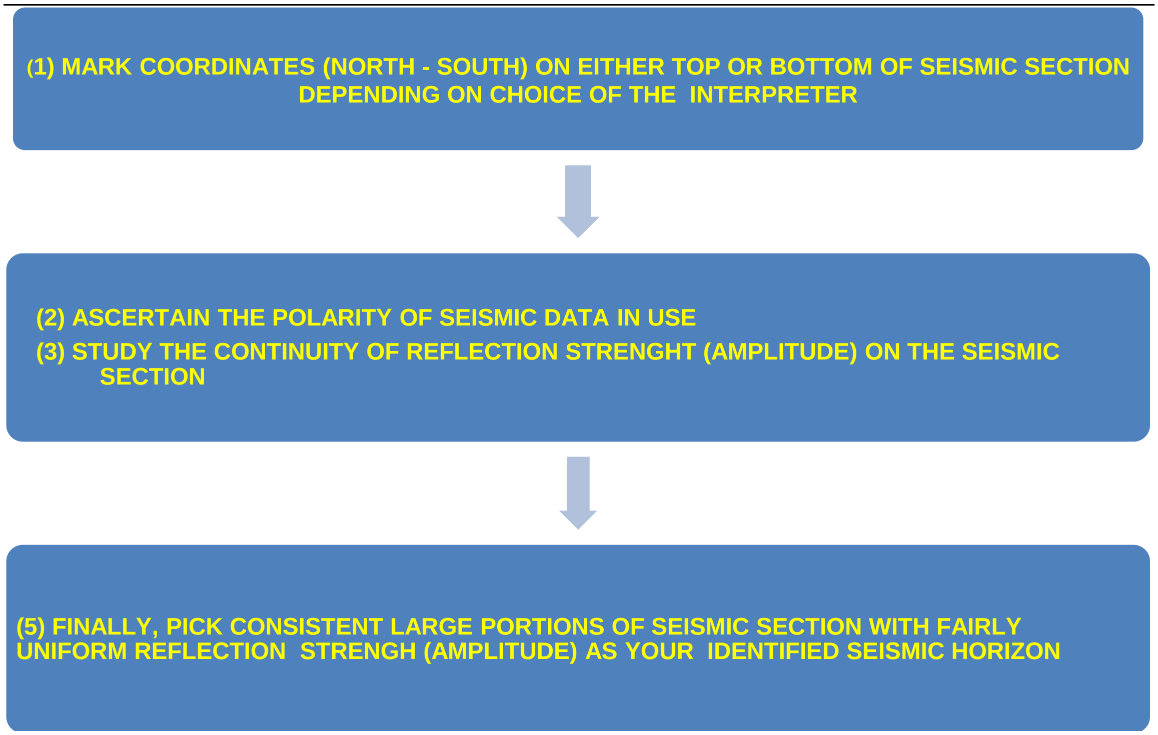

Figure 6. Workflow for the interpretation of seismic horizons on the seismic section.

closures with six prominent interpreted faults having good throws on inline 2770 (Figure 7). There are one major fault block F_1, four synthetic (growth) faults F_2, F_4, F_5, and F_6 that dips basin ward (SW) and one antithetic fault F_3 dipping landward (NW). The faults types and corresponding dip directions are shown in Table 1.

Three seismic horizons were mapped and designated as H1, H2, and H3 (Figure 8). The horizons were delineated at 1700, 1950 and 2250 ms, respectively, by laterally continuous reflection with medium-high amplitudes. These horizons are indications of top reservoir sands, which could be associated with both oil and gas with/without water contact. Subsequently, these were characterized in terms of their amplitude, reflection strength, reflection configuration and continuity (Table 2).

Furthermore, the interpreted faults and seismic horizons were extracted from the section to reveal the structural texture of the field and map possible fault closures for hydrocarbon accumulation (Figure 9). Results show that several fault assisted closures abound in the study area, which are potential sites for probable hydrocarbon accumulation.

DISCUSSION

Structural evaluation of a 3D PSTM seismic data from the southern part of an X-Field in the eastern onshore Niger Delta field has been attempted. The study revealed that the field is an E-W elongate rollover anticline structure bounded by growth faults. The field is comprised of both hanging wall/footwall fault assisted closures situated mostly to west and central parts of the section, with five prominent synthetic (F_1, F_2, F_4, F_5 and F_6) and one antithetic (F_3) growth faults. The synthetic faults trend NE-SW and dips southwestward, while the antithetic fault trend NW-SE and dips southeastward.

The fault closures are characterized by high amplitude reflection events indicative of probable hydrocarbon accumulation. Fairly high amplitudes and strong reflection strength are characteristic of the fault boundaries in the field. These are possible indications of the smearing of the faults and sealing of the reservoirs by clays or shales, which is adequate for trapping hydrocarbons within these fault closures. These revelations suggest that both gas and oil may be present in the field.

The study delineated three seismic horizons H_1, H_2 and H_3. H_1 is shallow while H_2 and H_3 horizons are deeply buried. The deeper horizons (H_2 and H_3) are fault truncated and have good fault closure for hydrocarbon trapping. This is true for H_2 and H_3 horizons with closures in-between faulted blocks along the inline. The major prospect is delineated mostly on the up thrown side of the major structure building faults beyond 1800 ms on the section along the seismic horizons H_2 and H_3.

The seismic horizons are characterized by reflections with moderate-strong reflection strength, medium-high amplitude, parallel-sub parallel-wavy and chaotic with

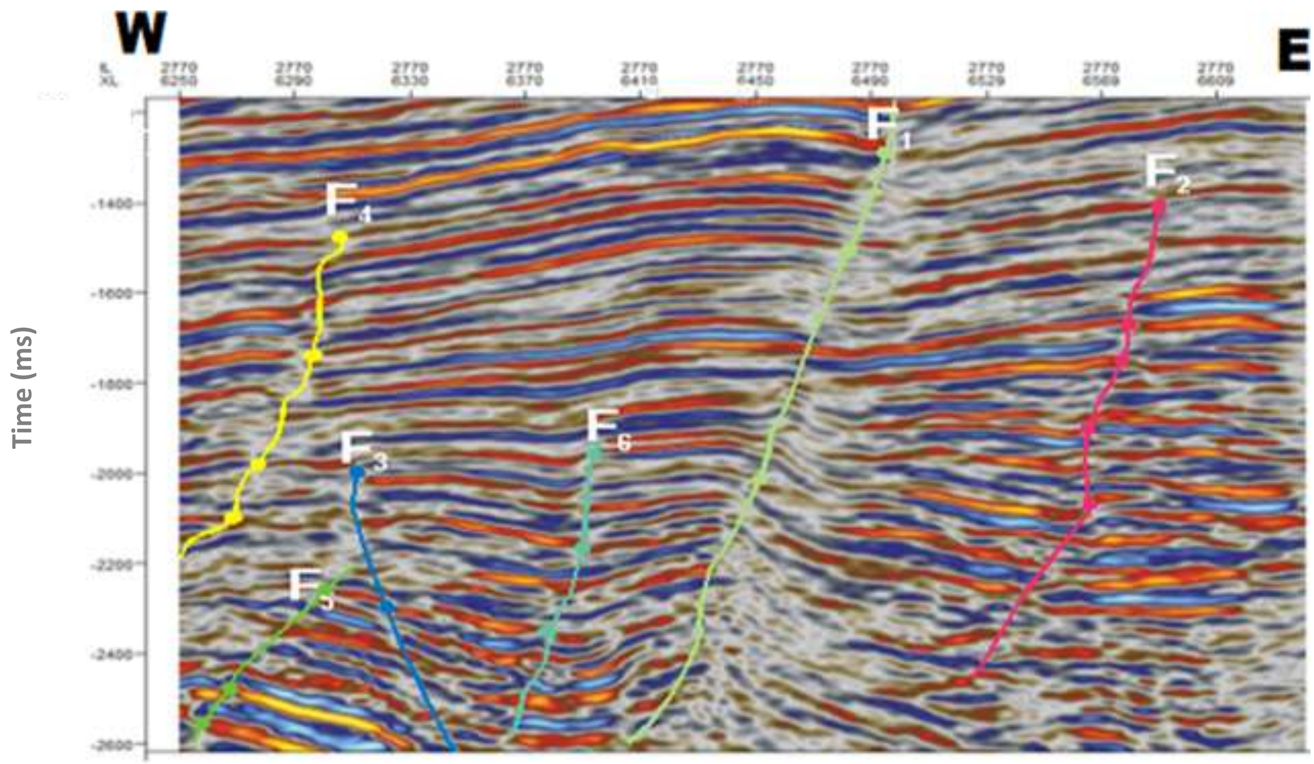

Figure 7. Seismic section showing the 6 interpreted faults (In line 2770).

Table 1. Interpreted faults classified according to types and dip direction.

Fault	Fault type	Dip Direction
F_1	Synthetic (major fault block)	South West
F_2	Synthetic (growth fault)	South West
F_3	Antithetic "	North West
F_4	Synthetic "	South West
F_5	Synthetic "	South West
F_6	Synthetic "	South West

good reflection continuity. This continuity in reflection suggests widespread and uniform deposition along the strike direction. Moderate-strong reflection strength implies a moderate variation in acoustic impedance contrast in the lithofacies, whereas the moderate to strong reflection and medium-high amplitude indicates thick sand body with inter-bedding shales (Figure 8), characteristic of a hydrocarbon reservoir in the Niger Delta basin.

However, recent studies by several authors in the Niger Delta (Ogboke, 2006; Oyedele et al., 2013; Obiekezie, 2014; Odoh et al., 2014), show that faults constitute the main structural trap for hydrocarbons in the basin. These authors attributed to the configuration and ability of the Delta fault systems to form closures enclosing thick reservoir sands with interbedded shale formations. They concluded that the presence of fault assisted structural closures are often times associated with probable hydrocarbon accumulations after detailed analysis of the seismic data.

The study area is a promising field with good structural framework for hydrocarbon trapping and accumulation. The majority of the faults in the field constitute the main structural trap for hydrocarbon accumulation. Thick reservoir sands with inter-bedded clays/shales within the fault bound closures characterize the field. The inter-bedded shales serve as good cap rocks to prevent vertical migration and seepage of hydrocarbons into overlaying sediment layers. The prospects for hydrocarbon is high in the field and this could be further ascertained by detailed quantitative analysis of 3D seismic and well log datasets prior to field development.

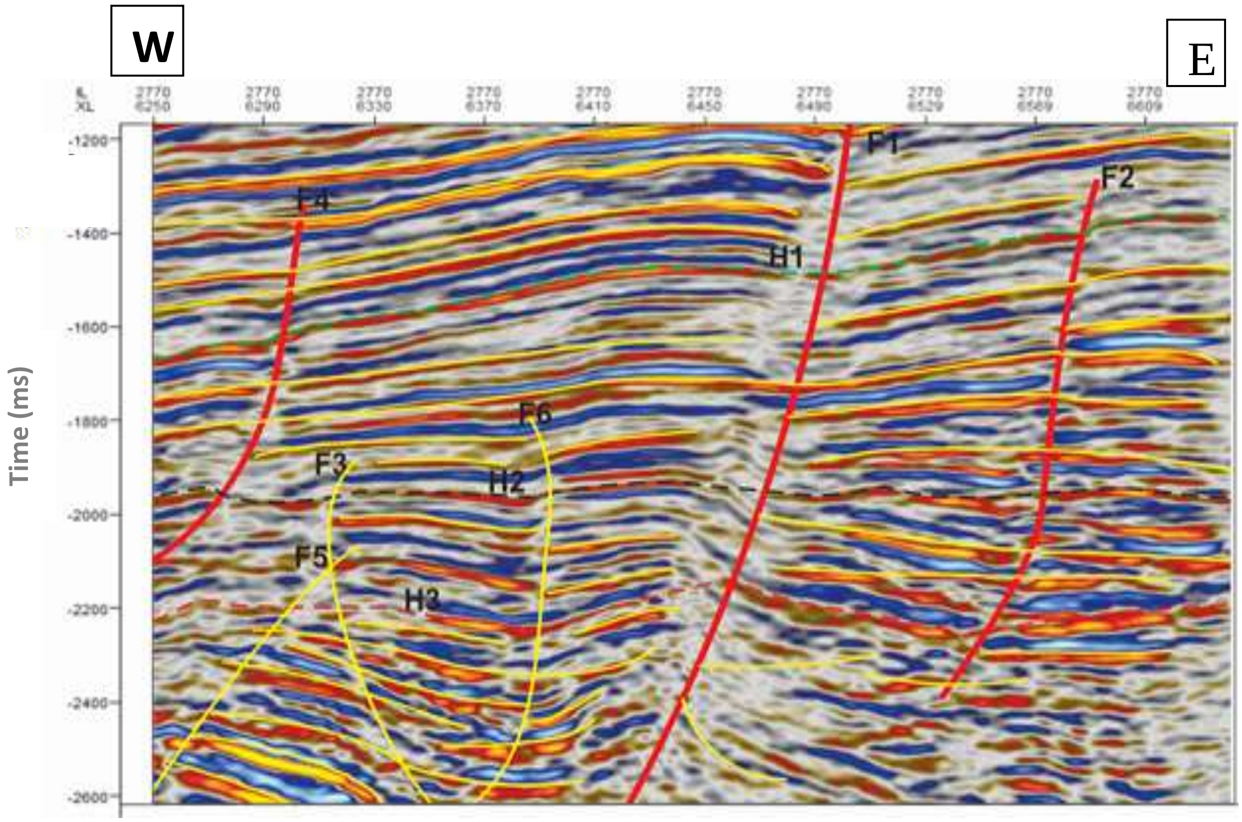

Figure 8. Seismic section showing the interpreted Faults and the three Seismic horizons (HI, H2 and H3).

Table 2. Interpreted attributes of the Seismic horizons.

Seismic horizon	Reflection strength	Amplitude	Configuration	Continuity
H_1	Moderate-Strong	Medium-High	Parallel-Sub parallel	High-good and fault truncated
H_2	Very Strong	High	Sub parallel-Wavy	High-good and fault truncated
H_3	Weak	Low	Sub parallel-Wavy	High-good, fault truncated and fairly chaotic to the west

Conclusion

A structural evaluation of a PSTM 3D seismic data have been presented along inline 2770 over an X-Field in the eastern Niger Delta. The X-field is a promising prospect with good structural frame work for hydrocarbon accumulations. Five synthetic and one antithetic growth faults with three seismic horizons were interpreted in the section.

The seismic horizons have fault assisted hanging wall/ footwall closures with distinctive high amplitude reflection events, which are indicative of probable hydrocarbon accumulation. The horizons are characterized by moderate to strong reflection strength, medium to high amplitudes and good reflection continuity. These suggests wide spread and uniform deposition of clastic sediments with thick sand facies and inter-bedding shales, which is characteristic of hydrocarbon reservoirs in the Niger Delta basin. The prospects for hydrocarbon in the field are high which can be explored.

Conflict of Interests

The authors have not declared any conflict of interests.

ACKNOWLEDGEMENTS

The authors are grateful to the donors of the seismic datasets used for this investigation (SPDC). It was anonymously donated for academic purpose/research only at the University of Port Harcourt.

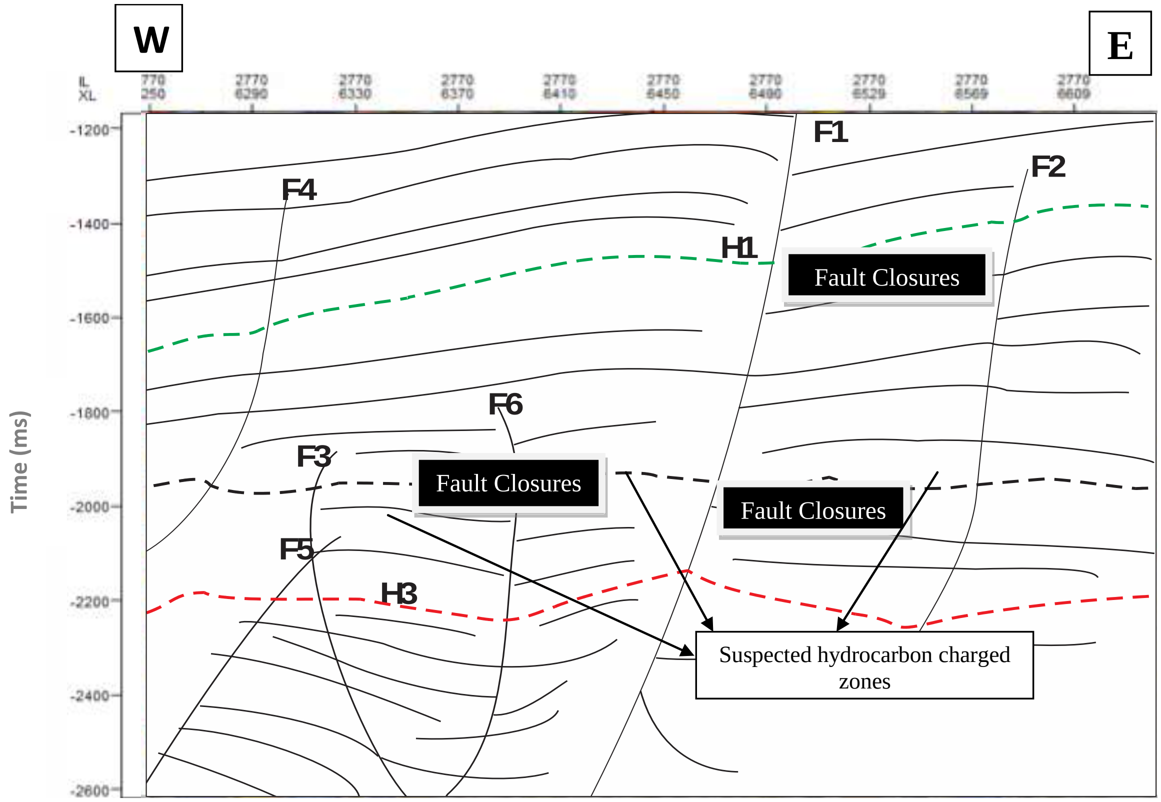

Figure 9. Interpreted section showing the Fault closures on the section.

REFERENCES

Adejobi AR, Olayinka AI (1997). Stratigraphy and hydrocarbon potential of the Opuama channel complex area, western Niger delta. Nig. Assoc. Pet. Explor. (NAPE) Bull. 12:1-10.

Aigbedion I, Iyayi SE (2006). An appraisal of the Abura field. Int. J. Phys. Sci. 2:93-100.

Allstair RB (2011). Interpretation of 3D seismic data (seventh edition). The American Association of Petroleum Geologists and Society of Exploration Geophysics, Tusla, Oklahoma, USA.

Anstey NA (1980). Seismic Exploration for sandstone reservoirs. Int. Human Res. Dev. Corp.

Avseth P, Mukerji T, Mavko G (2005). Quantitative seismic interpretation. Cambridge University Press pp. 168-170.

Bahorich M, Farmer S (1995). 3-D seismic discontinuity for faults and stratigraphic features: The coherence cube. Leading Edge 14:1053-1058.

Bouvier JD, Kaars-Sijpesteijn CH, Kluesner DF, Onyejekwe CC (1989). Three-Dimensional Seismic Interpretation and Fault Sealing Investigations. Nun River Field, Nigeria. AAPG bull. 73(11):1397-1414.

Doust H, Omatsola E (1989). Niger Delta: American Association of Petroleum Geologists Memoir 48:201-238.

Doust H, Omatsola E (1990). Niger Delta in Divergent / passive margin Basin, AAPG memoir 48; Tulsa. Am. Assoc. Pet. Geol. pp. 239-248.

Evamy BD, Haremboure J, Kamerling P, Knaap WA, Molloy FA, Roelands PH (1978). Hydrocarbon Habitat of Tertiary niger delta. Am. Assoc. Pet. Geol. Bull. 62:277-298.

McQuillin R, Bacon M, Barclay W (1984). An introduction to seismic interpretation: reflection seismic in petroleum exploration, Graham & Trotman Ltd. (2nd Ed.) London.

Obiekezie TN (2014). Hydrocarbon exploration in Odo field in the Niger delta basin Nigeria, using a 3-D seismic reflection survey. Sci. Res. Essays 9(17):778-784.

Odoh BI, Ilechukwu JN, Okoli NI (2014). The Use of Seismic Attributes to Enhance Fault Interpretation of OT Field, Niger Delta. Int. J. Geosci. 5:826-834.

Ogboke O (2006). Mapping of structural trap using 3D interpretation tool in Asin field, Niger Delta, Unpublic M.Sc. Thesis, University of Southern Venezuela.

Oyedele KF, Ogagarue DO, Mohammed DU (2013). Integration of 3D Seismic and Well log Data in the Optimal Reservoir Characterisation of EMI Field, Offshore Niger Delta Oil Province, Nigeria. Am. J. Sci. Ind. Res. 4(1):11-21.

Petters SW, Olsson RK (1979). Planktic Foraminifera from the Ewekoro Type Section (Paleocene). Nig. Micropaleontol. 25(2):206-213.

Sheriff RE, Geldart LP (1995). Exploration seismology: Press syndicate of the University of Cambridge P 592.

Short KC, Stauble AJ (1967). Outline of Geology of Niger Delta. Am. Assoc. Pet. Geol. Bull. 51:761-799.

Weber KJ, Daukoru EM (1975). Petroleum Geology of the Niger Delta: Proceedings of the Ninth World Petroleum Congress, 2, Geology: London. Appl. Sci. Pub. pp. 210-221.

International Journal of Physical Sciences

Related Journals Published by Academic Journals

- *African Journal of Pure and Applied Chemistry*
- *Journal of Internet and Information Systems*
- *Journal of Geology and Mining Research*
- *Journal of Oceanography and Marine Science*
- *Journal of Environmental Chemistry and Ecotoxicology*
- *Journal of Petroleum Technology and Alternative Fuels*